



PUBLISHED FOR SISSA BY SPRINGER

RECEIVED: May 18, 2012

ACCEPTED: June 15, 2012

PUBLISHED: July 5, 2012

Probing top-Higgs non-standard interactions at the LHC

C. Degrande,^{a,b} J.-M. Gérard,^b C. Grojean,^c F. Maltoni^b and G. Servant^{c,d}

^a*Department of Physics, University of Illinois at Urbana-Champaign,
1110 W. Green Street, Urbana, IL 61801, U.S.A.*

^b*Centre for Cosmology, Particle Physics and Phenomenology (CP3),
Chemin du Cyclotron 2, Université catholique de Louvain, Belgium*

^c*CERN Physics Department, Theory Division,
CH-1211 Geneva 23, Switzerland*

^d*Institut de Physique Théorique, CEA/Saclay,
F-91191 Gif-sur-Yvette Cédex, France*

E-mail: cdegrand@illinois.edu, jean-marc.gerard@uclouvain.be,
christophe.grojean@cern.ch, fabio.maltoni@uclouvain.be,
geraldine.servant@cern.ch

ABSTRACT: Effective interactions involving both the top quark and the Higgs field are among the least constrained of all possible (gauge invariant) dimension-six operators in the Standard Model. Such a handful of operators, in particular the top quark chromomagnetic dipole moment, might encapsulate signs of the new physics responsible for electroweak symmetry breaking. In this work, we compute the contributions of these operators to inclusive Higgs and $t\bar{t}h$ productions. We argue that: i) rather strong constraints on the overall size of these operators can already be obtained from the current limits/evidence on Higgs production at the LHC; ii) $t\bar{t}h$ production will provide further key information that is complementary to $t\bar{t}$ measurements, and the possibility of discriminating among different contributions by performing accurate measurements of total and differential rates.

KEYWORDS: Higgs Physics, Beyond Standard Model

ARXIV EPRINT: [1205.1065](https://arxiv.org/abs/1205.1065)

Contents

1	Introduction	1
2	Operators of interest	2
3	Higgs production by gluon fusion	3
4	$t\bar{t}h$ production	7
5	Conclusion	11
A	Explicit example with $c_{HG} \ll c_{hg}$	12

1 Introduction

The Standard Model (SM) has been tested with an impressive accuracy and is so far in excellent agreement with the experimental data. The room left for new physics at the TeV scale is therefore getting more and more squeezed, thanks to the LHC. Effective field theory (EFT) provides a model independent parametrization of the potential deviations from the SM while keeping its successes if the new degrees of freedom are heavy. EFT has been intensively used for instance in flavor physics to translate the accuracy of the measurements into strong constraints on the coefficients of the associated operators [1]. Slightly softer constraints on the operators involving weak bosons have also been derived from the electroweak precision measurements [2, 3]. In comparison, the operators involving the top quark are poorly constrained so far [4], especially the chromomagnetic moment operator of the top quark [5, 6], while those involving the Higgs field remain largely unconstrained. However, this status is about to change. In particular, modifications of the top quark interactions can significantly change the main Higgs production mechanism at hadron colliders, which is under scrutiny at the LHC.

In this paper, we focus on operators that involve both the top quark and the Higgs field. Not only they are little tested, but it is also where one might expect new physics associated with electroweak symmetry breaking to show up. First, we compute their contributions to $gg \rightarrow h$ due to a top loop. The only non-trivial contribution due to the chromomagnetic operator turns out to be finite and not logarithmic divergent as one would have expected by naive power counting. We then derive the constraints from the experimental bound on the Higgs production rate. Higgs production by gluon fusion alone does not allow to distinguish the new contributions since they are all proportional to the SM amplitude. In section 4, we argue that $t\bar{t}h$ production can provide complementary information to further constrain and to disentangle the various top-Higgs operators.

2 Operators of interest

Recently, constraints on effective Higgs interactions from the latest Higgs searches have been derived [7–13], with an emphasis on the $d = 6$ operators built from the Higgs and SM gauge bosons. These papers display global fits in a large parameter space. While ref. [8] and ref. [9], are restricted to a particular UV set-up where only a sub-class of operators are important, refs. [7, 10] included the modification of all Higgs interactions to the SM particles but considered that only the Yukawa coupling of the fermions were changed, and therefore have not considered the chromomagnetic operator. The spirit of this work is different in that our motivation is to focus only on $d = 6$ operators that involve both the Higgs field and the top quark. We study their effect on Higgs production by gluon fusion and associated with a $t\bar{t}$ pair, assuming in particular that hWW and hZZ tree-level couplings are not affected by new physics. The results of our analysis can easily be updated once the hWW and hZZ couplings are better determined. We start with the effective lagrangian [14–16]

$$\mathcal{L} = \mathcal{L}^{\text{SM}} + \sum \frac{c_i}{\Lambda^2} \mathcal{O}_i + O\left(\frac{1}{\Lambda^4}\right). \quad (2.1)$$

The chromomagnetic dipole moment operator modifies the interactions between the gluons and the top quark,

$$\mathcal{O}_{hg} = (\bar{Q}_L H) \sigma^{\mu\nu} T^a t_R G_{\mu\nu}^a, \quad (2.2)$$

where $\sigma^{\mu\nu} = \frac{i}{2} [\gamma^\mu, \gamma^\nu]$ and T^a is such that $\text{Tr}(T^a T^b) = \delta^{ab}/2$. Besides, one operator contains the top density

$$\mathcal{O}_{Hy} = H^\dagger H (H \bar{Q}_L) t_R \quad (2.3)$$

and three operators can be built from the top and Higgs currents,

$$\begin{aligned} \mathcal{O}_{Ht} &= H^\dagger D_\mu H \bar{t}_R \gamma^\mu t_R \\ \mathcal{O}_{HQ} &= H^\dagger D_\mu H \bar{Q}_L \gamma^\mu Q_L \\ \mathcal{O}_{HQ}^{(3)} &= H^\dagger \sigma^I D_\mu H \bar{Q}_L \sigma^I \gamma^\mu Q_L. \end{aligned} \quad (2.4)$$

Other operators of dimension 6 play a role in the top-Higgs interaction even though they do not contain both fields. One of them is

$$\mathcal{O}_H = \partial_\mu (H^\dagger H) \partial^\mu (H^\dagger H), \quad (2.5)$$

which amounts to an overall renormalization of the Higgs wave function and therefore to a trivial shift of the top-quark Yukawa coupling [17].

The corrections from those operators to Higgs production by gluon fusion are shown in figure 1. In the large top mass limit, the contribution of the operators in eqs. (2.2), (2.3) can be seen as corrections to the \mathcal{O}_{HG} operator

$$\mathcal{O}_{HG} = \frac{1}{2} H^\dagger H G_{\mu\nu}^a G_a^{\mu\nu} \quad (2.6)$$

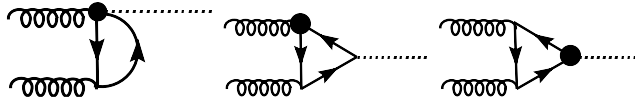


Figure 1. $gg \rightarrow h$ production. The first two diagrams are the contributions to \mathcal{O}_{HG} from \mathcal{O}_{hg} . The third one is induced by $\mathcal{O}_{H\gamma}$ and \mathcal{O}_H . The operators of eq. (2.4) do not contribute to \mathcal{O}_{HG} (see section 3).

generated by the scale anomaly. Therefore, we are going to derive the constraints on \mathcal{O}_{HG} from Higgs production, which we will then re-express in terms of limits on a combination of the above operators.

One should remark that not only the Higgs production rate is sensitive to the modifications of the top interactions but also the $h \rightarrow \gamma\gamma$ decay. The operator \mathcal{O}_H does not change the branching ratios since it multiplies all partial widths by the same factor. However, $\mathcal{O}_{H\gamma}$ and the electromagnetic version of \mathcal{O}_{hg} induce

$$\mathcal{O}_{H\gamma} = \frac{1}{2} H^\dagger H F_{\mu\nu} F^{\mu\nu}. \quad (2.7)$$

The main effect of this operator will be to relax the constraints from the $h \rightarrow \gamma\gamma$ channel. We reiterate that we do not consider corrections to hWW and hZZ vertices. New top interactions affect all these channels at one-loop. However, their effects to the loop-induced processes $h \rightarrow \gamma\gamma$ and $gg \rightarrow h$ are expected to be relatively larger than for $h \rightarrow WW$ and $h \rightarrow ZZ$ because the new operators modify the SM leading order in the first case and the NLO corrections in the second.

3 Higgs production by gluon fusion

\mathcal{O}_{HG} is the only dimension-six operator inducing Higgs production by gluon fusion at tree-level. Its effect on the partonic cross-section is (see also refs. [18, 19])

$$\sigma(gg \rightarrow h) = \sigma(gg \rightarrow h)_{\text{SM}} \left(1 + \frac{c_{HG}}{\Lambda^2} \frac{6\pi v^2}{\alpha_s} \right)^2, \quad (3.1)$$

where we have taken the heavy top limit for the SM, i.e., $m_t > m_H/2$, and $v \approx 246$ GeV is the Higgs vacuum expectation value (vev). The contribution from \mathcal{O}_{HG} is quite large compared to the SM one ($6\pi v^2/\alpha_s \sim 10 \text{ TeV}^2$) because the latter is only generated at the loop-level. Consequently, the upper limits on the Higgs production cross-section from the Tevatron [20] and the LHC [21–23] strongly constrain the allowed range for c_{HG} , as shown on figure 2. For this figure, we assume that only \mathcal{O}_{HG} is added to the SM Lagrangian, i.e., we neglect the modifications of the other production mechanisms or of the decay widths except for $h \rightarrow gg$. We used the same NNLO K factor for the contribution of the \mathcal{O}_{HG} as for the SM [24] since both amplitudes are the same up to a global factor. The errors on these limits have been estimated by varying simultaneously the renormalization (μ_R) and factorization scales (μ_F) for the SM and the \mathcal{O}_{HG} tree-level contributions. Other theoretical

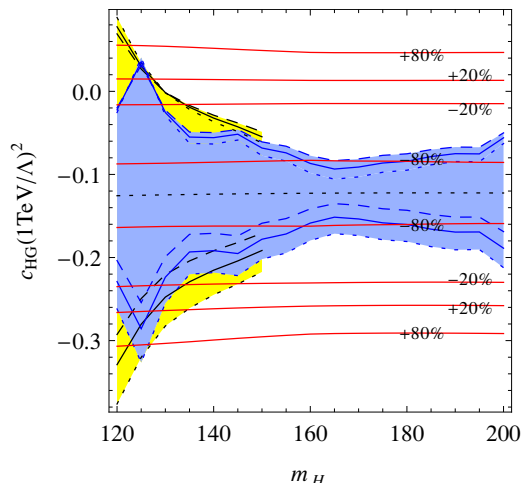


Figure 2. Region allowed at 95% C.L. by the ATLAS upper bound on the Higgs production cross-section [23] for $\mu_R = \mu_F = m_H/2$ (solid line). The errors are estimated by varying the renormalization and factorization scales from $\mu_R = \mu_F = m_H/4$ (dotted line) to $\mu_R = \mu_F = m_H$ (dashed line). The blue region uses the combination of all channels. The yellow region is obtained using the strongest constraint among the WW and ZZ channels. The red lines show the relative deviation compared to the SM Higgs production rate.

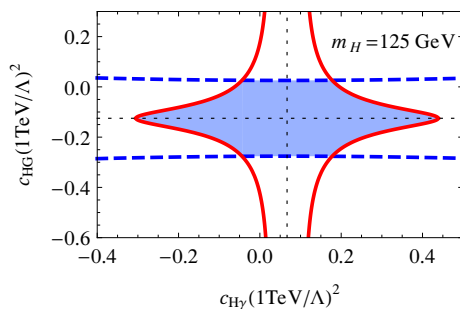


Figure 3. The dashed blue and solid red lines are the limits from $h \rightarrow (WW, ZZ)$ and $h \rightarrow \gamma\gamma$ respectively. The WW/ZZ constraints on c_{HG} are stronger only when the branching ratio to $\gamma\gamma$ goes below 10^{-3} (SM value), corresponding to $0 \lesssim c_{H\gamma} \lesssim 0.1$. For larger branching ratio, the $\gamma\gamma$ constraints are stronger and do not allow for large values of $c_{H\gamma}$. Note that the allowed region is symmetric along the dotted black lines where $\sigma(gg \rightarrow h) = 0$ and $\Gamma(h \rightarrow \gamma\gamma) = 0$. We have checked that a more refined analysis combining all the channels along the lines of ref. [9] gives qualitatively similar results, although slightly more constraining of course.

errors are much smaller. For $m_H = 125$ GeV, we obtain $-0.29 \lesssim c_{HG}(\text{TeV}^2/\Lambda^2) \lesssim 0.036$. We also show in yellow how the constraints on c_{HG} are relaxed when including the effect of $\mathcal{O}_{H\gamma}$. The exclusion in the plane $(c_{HG}, c_{H\gamma})$ is shown in figure 3. Again, figure 2 is valid only for SM hWW and hZZ couplings but a similar plot can be drawn once the actual values of hWW and hZZ will be determined.

The constraints on c_{HG} of figure 2 translate into constraints on a combination of the coefficients of the operators eqs. (2.2)–(2.5). The one-loop correction from \mathcal{O}_{hg} to the

operator \mathcal{O}_{HG} is expected to diverge logarithmically since both operators are of dimension-six. However, its one-loop contribution is finite [25] and can be written as

$$\delta c_{HG} = \frac{g_s y_t}{4\pi^2} \Re c_{hg} \left(1 - \frac{m_H^2}{24m_t^2} + O\left(\left(\frac{m_H}{2m_t}\right)^4\right) \right) \quad (3.2)$$

since the dependence on m_H is very weak for a light Higgs boson. To derive eq. (3.2), we consistently use dimensional regularization in the intermediate steps of the calculation.

The operators \mathcal{O}_{Hy} and \mathcal{O}_H renormalize the top mass

$$m_t = y_t \frac{v}{\sqrt{2}} - \frac{\Re(c_{Hy}) v^3}{2\sqrt{2} \Lambda^2} \quad (3.3)$$

and/or the top Yukawa coupling,

$$\begin{aligned} \mathcal{L}^{ht\bar{t}} &= \bar{t}t \frac{h}{\sqrt{2}} \left(y_t - \left(\frac{3}{2} \Re(c_{Hy}) + y_t c_H \right) \frac{v^2}{\Lambda^2} \right) \\ &= \bar{t}t h \frac{m_t}{v} \left(1 - c_y \frac{v^2}{\Lambda^2} \right), \end{aligned} \quad (3.4)$$

where

$$c_y = c_H + \frac{v}{\sqrt{2}m_t} \Re(c_{Hy}) . \quad (3.5)$$

Their contributions are then easily obtained as a simple rescaling of the SM contribution [17, 26]

$$\frac{\delta c_{HG}}{\Lambda^2} = \frac{\alpha_s}{6\pi v^2} \times \left(-c_y \frac{v^2}{\Lambda^2} \right). \quad (3.6)$$

The other three operators listed in eq. (2.4) do not contribute to Higgs production by gluon fusion. In fact, the vertex $ht\bar{t}$ comes from the sum of those operators and of their Hermitian conjugates.¹ The relevant part of the operators can thus be written as

$$\begin{aligned} \partial_\mu \left(H^\dagger H \right) \bar{t} \gamma^\mu \gamma_{\pm t} t &\propto \left(H^\dagger H \right) \partial_\mu \frac{(J^\mu \pm J_5^\mu)}{2} \\ &\propto \left(H^\dagger H \right) \partial_\mu J_5^\mu \end{aligned} \quad (3.7)$$

because the vector current is conserved. Their contributions to Higgs production through the effective operator $H^\dagger H G^{\mu\nu} \tilde{G}_{\mu\nu}$, generated by the axial anomaly, vanish in the SM due to parity. This result is consistent with the operator relations derived in ref. [27]. In Two-Higgs-Doublet-Models with a light pseudo-scalar, this effective operator should be taken into account [28].

Taking $m_t = 174.3 \text{ GeV}$, $m_H = 125 \text{ GeV}$, $v = 246 \text{ GeV}$ and $g_s = 1.2$, we obtain

$$\delta c_{HG} \approx 0.03 \Re c_{hg} - 0.006 c_y. \quad (3.8)$$

¹This combination is invariant under custodial symmetry and can thus not be constrained by the ρ parameter.

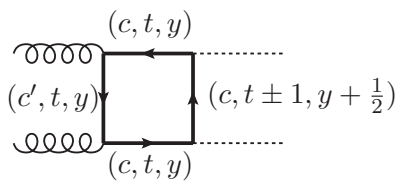


Figure 4. Diagram leading to the operator \mathcal{O}_{HG} with the particles in the loop labeled by their transformations under $SU(3) \times SU(2) \times U(1)$, i.e., (c, T, Y) if $\bar{c} \otimes c' \ni 8$. If the particles in the loop are bosons, additional diagrams can be obtained by replacing one or two internal lines and their two adjacent vertices by a single vertex.

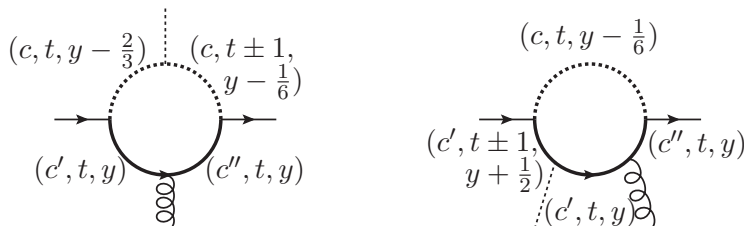


Figure 5. Diagrams leading to the operator \mathcal{O}_{hg} if $\bar{c}' \otimes c'' \ni 8$, $\bar{c} \otimes c' \ni 3$ and $\bar{c} \otimes c'' \ni 3$. The internal fermion and boson lines can be exchanged and the internal bosons do not have to be scalar. Similarly as for figure 4, additional diagrams can be obtained by removing one internal boson propagator.

Even if the effects due to the new interactions of the top quark are loop suppressed, they cannot be neglected. The coefficient c_y , probing the relation between the top mass and its Yukawa coupling, is not constrained by any other process than Higgs production (see recent and rather weak constraints on $c = 1 - c_y(v/\Lambda)^2$ in refs. [8, 9]). Similarly, the present constraints on c_{hg} due to top pair production [5] including the latest ATLAS combination [29], i.e., $-0.75 \lesssim c_{hg}(\text{TeV}/\Lambda)^2 \lesssim 3$ at 1σ and $-1.2 \lesssim c_{hg}(\text{TeV}/\Lambda)^2 \lesssim 3.5$ at 2σ , still allow the contribution from the chromomagnetic operator to have a noticeable effect on the allowed range for c_{HG} as will be illustrated in the summary plots of section 4.

The next question concerns the typical expectation for the size of the coefficient c_{HG} . For example, the one-loop contributions from \mathcal{O}_H and \mathcal{O}_{Hy} have been shown to be as large as the \mathcal{O}_{HG} contribution in little Higgs models [26]. The reason is that those operators \mathcal{O}_H and \mathcal{O}_{Hy} can be induced by the tree-level exchange of a heavy particle while \mathcal{O}_{HG} is only generated at the loop-level in a perturbative UV completion of the SM (see figure 4). The operator \mathcal{O}_H is also enhanced compared to \mathcal{O}_{HG} in strongly interacting Higgs models [17].

On the contrary, the chromomagnetic operator can hardly be enhanced. It is also generated only at the loop-level (see figure 5) in perturbation theory and thus for \mathcal{O}_{hg} to be the dominant new physics effects requires \mathcal{O}_{HG} to be relatively suppressed. While the diagram of figure 4 can be obtained by using twice the lower part of the second diagram in figure 5, the first diagram in figure 5 with $c = 1$ does not imply the presence of \mathcal{O}_{HG} . As a consequence, it is possible to generate the chromomagnetic operator, \mathcal{O}_{hg} , at one-

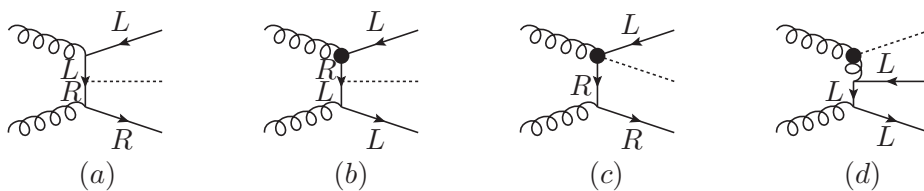


Figure 6. Examples of diagrams for $t\bar{t}h$ production from the SM (a), from the chromomagnetic operator \mathcal{O}_{hg} (b) and (c) and from the \mathcal{O}_{HG} operator (d). \mathcal{O}_H and \mathcal{O}_{Hy} lead to a simple rescaling of the SM contribution.

loop and not the operator \mathcal{O}_{HG} . An explicit example is given in appendix A. While dominant in this example, the effects from the chromomagnetic operator are too small to be observed. Alternatively, the hierarchy may come from strongly coupled theories and can be estimated with the help of Naive Dimensional Analysis [30, 31]. If only the right-handed top is strongly coupled, the dominant operator involves four top quarks yet does not contribute even at two-loop [32]. In that case, the coefficient of the chromomagnetic operator is only suppressed by one power of the strong coupling compared to two for c_{HG} and both operators can have similar contribution when the strong coupling approaches 4π . However, its effects may again be too small to be observed. So, let us now move to study the effect of these operators on $t\bar{t}h$ production.

4 $t\bar{t}h$ production

While both Higgs direct coupling to the gluons and new top interactions significantly affect Higgs production, they cannot be distinguished using this process only. Contrary to Higgs production by gluon fusion, the four operators \mathcal{O}_{HG} , \mathcal{O}_{hg} , \mathcal{O}_H and \mathcal{O}_{Hy} all contribute to $t\bar{t}h$ at the tree-level (see figure 6). Again, the three operators in eq. (2.4) have no contribution for this process due to parity. There is only one additional operator affecting this process,

$$\mathcal{O}_G = f^{ABC} G_\mu^{A\nu} G_\nu^{B\rho} G_\rho^{C\mu}. \quad (4.1)$$

However, this operator involves neither the top quark nor the Higgs boson and is thus not expected to be enhanced. Moreover, the interference between \mathcal{O}_G and the SM has a suppression similar to that associated with the octet exchange in top pair production ($\propto \beta^2 m_t^2$) [33]. Indeed, the contribution proportional to c_G in the squared amplitude for $gg \rightarrow t\bar{t}h$ vanishes at threshold and becomes constant at large s . Large shape effects on energy dependent distributions are thus not expected from this operator. Consequently, although we include this operator in the calculation of the cross section, we do not consider it in our phenomenological analysis and set $c_G = 0$ in all plots. The four-fermion operators cannot modify the main process, i.e., gluon fusion. Consequently, their contributions are about one order of magnitude smaller and have not been included. The contribution from \mathcal{O}_H and \mathcal{O}_{Hy} , being just a rescaling of the top Yukawa coupling (see eqs. (3.4) and (3.5)), is proportional to the SM cross section:

$$\sigma(pp \rightarrow t\bar{t}h) = \sigma(pp \rightarrow t\bar{t}h)_{\text{SM}} \left(1 - c_y \frac{v^2}{\Lambda^2}\right)^2 \quad (4.2)$$

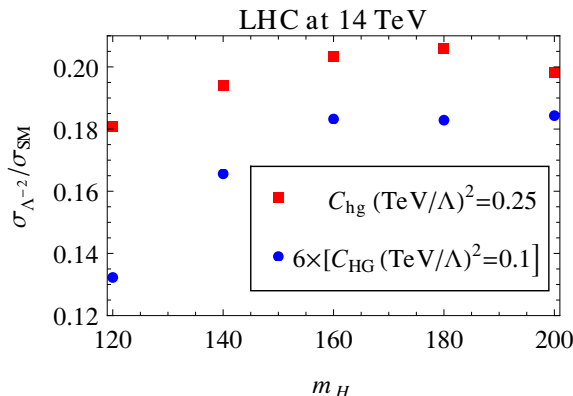


Figure 7. Ratio of the interference (between the SM and the main dimension-six operators) and the SM $pp \rightarrow t\bar{t}h$ cross section as a function of the Higgs mass. CTEQ611 pdf set and $\mu_R = \mu_F = m_t = 174.3$ GeV are used and the results are very similar at 7 TeV.

and this relation holds at NLO (at least in the flavor universal limit). The total cross-section at 14 TeV is given by

$$\begin{aligned} \frac{\sigma(pp \rightarrow t\bar{t}h)}{\text{fb}} &= 611_{-110}^{+92} + [457_{-91}^{+127} \Re c_{hg} - 49_{-10}^{+15} c_G + 147_{-32}^{+55} c_{HG} - 67_{-16}^{+23} c_y] \left(\frac{\text{TeV}}{\Lambda}\right)^2 \\ &+ [543_{-123}^{+143} (\Re c_{hg})^2 + 1132_{-232}^{+323} c_G^2 + 85.5_{-21}^{+73} c_{HG}^2 + 2_{-0.5}^{+0.7} c_y^2 - 50_{-14}^{+16} \Re c_{hg} c_y \\ &+ 233_{-144}^{+81} \Re c_{hg} c_{HG} - 3.2_{-8}^{+8} \Re c_{Hy} c_{HG} - 1.2_{-8}^{+8} c_H c_{HG}] \left(\frac{\text{TeV}}{\Lambda}\right)^4, \end{aligned} \quad (4.3)$$

at 8 TeV by

$$\begin{aligned} \frac{\sigma(pp \rightarrow t\bar{t}h)}{\text{fb}} &= 128 + [94 \Re c_{hg} - 9.7 c_G + 27 c_{HG} - 15 c_y] \left(\frac{\text{TeV}}{\Lambda}\right)^2 \\ &+ [53.9 (\Re c_{hg})^2 + 137 c_G^2 + 9.6 c_{HG}^2 + 0.4 c_y^2 + 19.3 \Re c_{hg} c_{HG} \\ &- 9.6 \Re c_{hg} c_y - 1.2 \Re c_{Hy} c_{HG} - 0.7 c_H c_{HG}] \left(\frac{1 \text{TeV}}{\Lambda}\right)^4, \end{aligned} \quad (4.4)$$

and at 7 TeV by

$$\begin{aligned} \frac{\sigma(pp \rightarrow t\bar{t}h)}{\text{fb}} &= 86.3_{-15}^{+10} + [63_{-14}^{+20} \Re c_{hg} - 5.6 c_G + 22.3_{-7}^{+8} c_{HG} - 10.2_{-2.5}^{+4} c_y] \left(\frac{\text{TeV}}{\Lambda}\right)^2 \\ &+ [43.6_{-12}^{+17} (\Re c_{hg})^2 + 78.3 c_G^2 + 8.6_{-3}^{+1} c_{HG}^2 + 0.3 c_y^2 + 21_{-2}^{+6} \Re c_{hg} c_{HG} \\ &- 7.2_{-1.7}^{+1} \Re c_{hg} c_y - 1.5_{-1}^{+1} \Re c_{Hy} c_{HG} - 1.1_{-1}^{+1} c_H c_{HG}] \left(\frac{\text{TeV}}{\Lambda}\right)^4, \end{aligned} \quad (4.5)$$

for $m_H = 125$ GeV. We included c_G and c_G^2 terms for indication (but not $c_G c_i$ terms), however, as mentioned earlier, we will set $c_G = 0$ in the rest of the analysis. The same factorization and renormalization scales as for top pair production, i.e., $\mu_F = \mu_R = m_t$ have been used since we have only considered a light Higgs boson. The cross-section will slightly decrease if higher values taking into account the Higgs mass are chosen. The errors

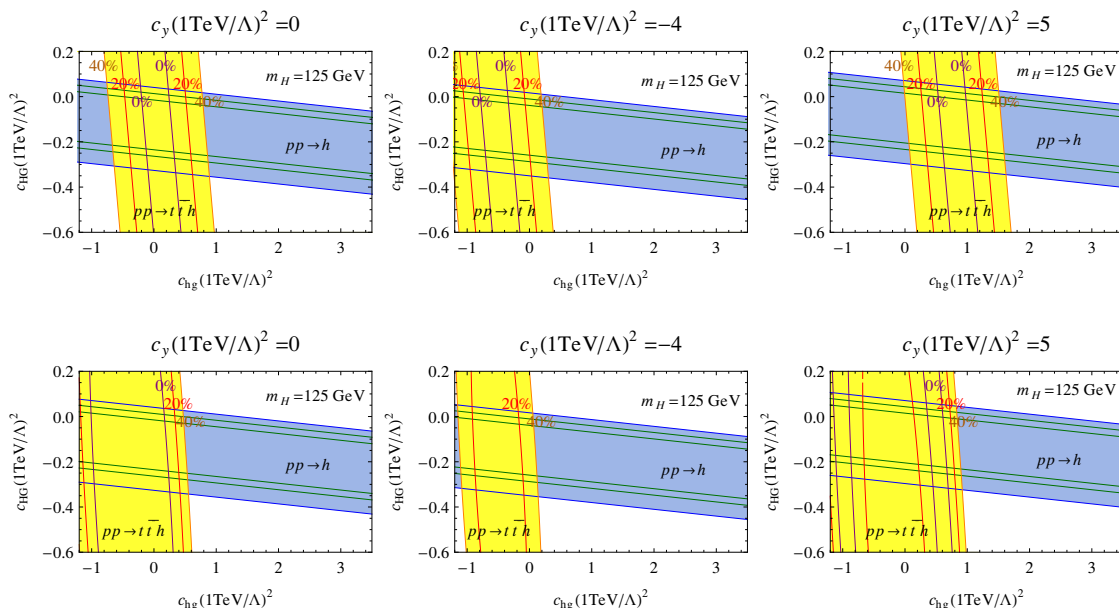


Figure 8. In blue, the region allowed by the Higgs production constraints at 7 TeV for $m_H = 125$ GeV. The green lines delimit the 2 allowed tiny bands obtained if the Higgs cross-section is measured at its SM value with a precision of 20 %. The yellow region is obtained by assuming a 40% precision on the $t\bar{t}h$ cross-section at 14 TeV with the measured central value matching the SM prediction and $c_G = 0$. The three plots correspond respectively to $c_y(\text{TeV}/\Lambda)^2 = 0, -4, +5$. The upper plots are obtained when neglecting the $\mathcal{O}(1/\Lambda^4)$ terms in the $t\bar{t}H$ cross section. The bottom plots instead include these higher order terms.

are again obtained by varying the factorization and renormalization scales simultaneously from $\mu_F = \mu_R = m_t/2$ to $\mu_F = \mu_R = 2m_t$, except for the last two terms $\Re(c_{Hy})c_{HG}$ and $c_{HC}c_{HG}$ for which the numerical errors are larger. Results have been obtained via the FeynRules-MadGraph 5 simulation chain [34–37]. The new physics has been computed at the tree-level and the SM contribution at NLO [24, 38, 39]. The $\mathcal{O}(1/\Lambda^4)$ terms have been computed to check the $1/\Lambda$ expansion and only take into account the operators that contribute also at the $1/\Lambda^2$ order, i.e., contain either squares of the operators $\mathcal{O}(1/\Lambda^2)$ or the interference of the SM with an amplitude involving two new vertices. Additional contributions from the operators in eq. (2.4) or dimension-eight operators and proportional to the imaginary part of c_{Hy} or c_{hg} are not included. The values of the $1/\Lambda^4$ coefficients tell us that the $1/\Lambda$ expansion breaks down around the TeV for $c_i = 1$. This lower value compared to top pair production [5] is expected due to the higher energy required for this final state. While eqs. (4.3)–(4.5) have been obtained only for a particular value of the Higgs mass, the ratios of the new physics contributions over the SM do not change drastically with the Higgs mass as shown on figure 7.

As shown by eqs. (4.3)–(4.5) and figure 7, $t\bar{t}$ associated Higgs production can mainly be affected by the chromomagnetic operator. As a consequence, the constraints from a measurement of the $t\bar{t}h$ cross-section would complement those from Higgs production as

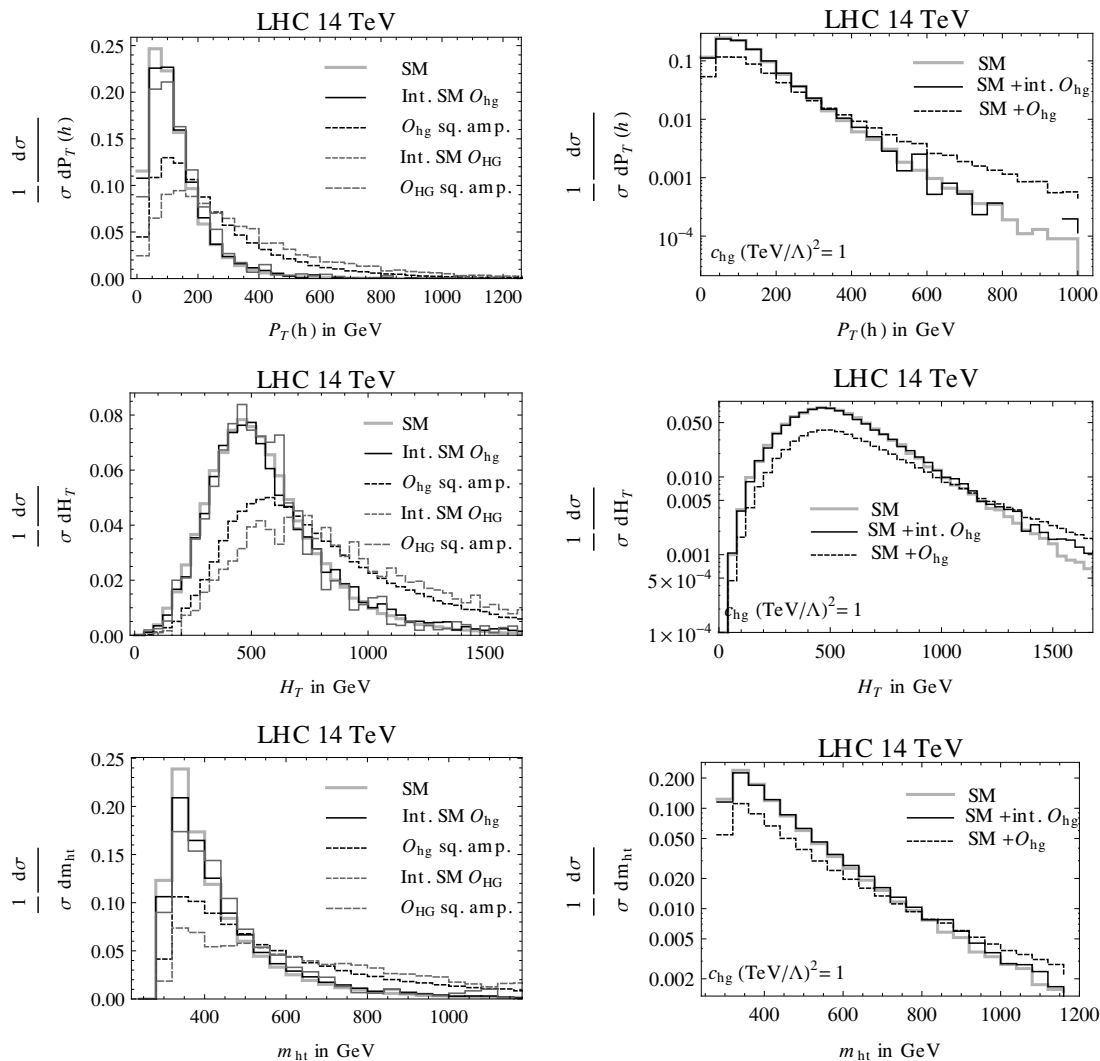


Figure 9. Left: Normalized distributions of the Higgs transverse momentum $P_T(h)$, the total H_T and the invariant mass of the Higgs-top system using CTEQ611 pdf set, $\mu_R = \mu_F = m_t = 174.3 \text{ GeV}$ and $m_H = 125 \text{ GeV}$ for the SM, its interference with O_{hg} and O_{HG} and the squared of the amplitudes with one effective vertex. These plots do not depend on the value of c_{hg} and c_{HG} . Right: Total contribution (SM + O_{hg}) for $c_{hg}(\text{TeV}/\Lambda)^2 = 1$ including the interference terms only and including both the interference terms and the terms of order $1/\Lambda^4$, compared to the SM only.

illustrated in figure 8, which displays the c_{hg} range allowed by the present measurements of the $t\bar{t}$ cross section. By the time the $t\bar{t}h$ cross section will be measured, the improved constraints from $t\bar{t}$ measurements will also help in reducing further the allowed range for c_{hg} according to ref. [5]:

$$\delta\sigma_{pp \rightarrow t\bar{t}}|_{14 \text{ TeV}} = 144 c_{hg} \left(\frac{\text{TeV}}{\Lambda}\right)^2 + 22.5 c_{hg}^2 \left(\frac{\text{TeV}}{\Lambda}\right)^4. \quad (4.6)$$

Like for top pair production, the theoretical uncertainty is responsible for a sizable part of the allowed region. Since those errors mainly affect the overall normalisation, this

issue could be solved by measuring the shapes of the distributions. Additionally, shape effects could also lift the remaining degeneracy between the four operators. While the contributions of the operators \mathcal{O}_{Hy} and \mathcal{O}_H have the same shapes as the SM ones, the operators \mathcal{O}_{hg} and \mathcal{O}_{HG} can induce shape distortions. However, only the contribution of the chromomagnetic operator might have a higher energy dependence than the SM. If the Higgs leg is attached to the effective vertex, the diagrams contain only one chirality flip such that no other chirality flip is needed to interfere with the SM amplitude (figure 6(c)). Moreover, the vertex is not proportional to the Higgs vev like for top pair production. Those advantages are lost if the Higgs is attached to the top line or to a gluon (figures 6(b) and (d)). For those diagrams, the amplitude is proportional to m_t and v and no room is left for extra powers of the energy of the process.

The distributions of the transverse momentum of the Higgs, the total H_T and the invariant mass of the Higgs-top system are displayed on figure 9. The shapes of the $1/\Lambda^4$ contributions are also shown for comparison. They are clearly stretched to high energy while the interference and the SM contributions have a very similar behavior. The interference with the diagrams in which the Higgs is connected at the effective vertex do not vanish but are apparently suppressed. The shape effects are only expected if the new physics scale Λ is close to the maximal energy probed because they are due only to the $1/\Lambda^4$ contributions. The plots on the right show how the distributions can differ with respect to the SM in the case $c_{hg}(\text{TeV}^2/\Lambda^2) = 1$.

Finally, spin correlations could exhibit some dependence on c_{hg} . In the case of $t\bar{t}$ production, the deviations due to c_{hg} were of the order of a few percents [5]. For $t\bar{t}h$, the measurement will be much more challenging and we therefore do not compute the associated spin correlations here but might return to them in due time.

5 Conclusion

Only one dimension-six operator, \mathcal{O}_{HG} , generates a tree level coupling between the Higgs boson and the gluons. This operator has the largest contribution to Higgs production. Nevertheless, the three operators modifying the contribution from the top loop also have sizable effects compared to the SM one and, in a large class of models, can be comparable to the effect of \mathcal{O}_{HG} due to the hierarchy between their coefficients. All those operators are already constrained by the present limits on Higgs production at hadron colliders. However, Higgs production by gluon fusion only constrains a linear combination of these operators and cannot discriminate between them. Interestingly, a light Higgs makes real the possibility of partially solving this issue by using Higgs production in association with a pair of top quarks. Contrary to Higgs production, the leading contribution in this process comes from the chromomagnetic operator \mathcal{O}_{hg} , which can therefore be further constrained from the measurement of the total $t\bar{t}h$ cross-section. Shape effects do not come from the interference terms and are dominated by the square of the amplitude involving an effective vertex and could thus be observable for large c_{hg} values only.

Acknowledgments

The work of C.D., J.-M. G. and F.M. is supported by the Belgian Federal Office for Scientific, Technical and Cultural Affairs through the Interuniversity Attraction Pole No. P6/11. C.D. is a fellow of the Fonds National de la Recherche Scientifique and the Belgian American Education Foundation. G.S is supported by the ERC Starting Grant 204072. C.G. is partly supported by the European Commission under the ERC Advanced Grant 226371 MassTeV and the contract PITN-GA-2009-237920 UNILHC. We thank D. Choudhury and P. Saha for useful discussions about the contribution of the chromomagnetic operator in $gg \rightarrow h$.

A Explicit example with $c_{HG} \ll c_{hg}$

In this appendix, we provide a toy model in which the diagrams of figure 5 are generated while the diagram of figure 4 is not. The new sector is given by

$$\begin{aligned} T_{L,R} &\sim (3, 1, Y) \\ \Phi &\sim (1, 2, Y - 1/6) \\ S &\sim (1, 1, Y - 2/3) \end{aligned} \tag{A.1}$$

where $Y \neq 2/3$ to avoid the mixing of T with the SM top and $Y \neq -1/3$ to avoid the mixing between Φ and the Higgs doublet. The extra piece of the Lagrangian is given by

$$\begin{aligned} \mathcal{L}^{\text{NP}} &= i\bar{T}\not{D}T - M\bar{T}T - \kappa \left(\bar{T}_R Q_L \Phi + \bar{Q}_L T_R \Phi^\dagger \right) - \beta \left(\bar{t}_R T_L S^\dagger + \bar{T}_L t_R S \right) + D_\mu S^\dagger D^\mu S \\ &\quad - M_S^2 S^\dagger S + \lambda_1 \left(S^\dagger S \right)^2 + \lambda_2 S^\dagger S H^\dagger H + \lambda_3 S^\dagger S \Phi^\dagger \Phi + D_\mu \Phi^\dagger D^\mu \Phi - M_\Phi^2 \Phi^\dagger \Phi \\ &\quad + \lambda_4 \left(\Phi^\dagger \Phi \right)^2 + \lambda_5 \Phi^\dagger \Phi H^\dagger H + M_3 \left(\Phi^\dagger H^\dagger S + H \Phi S^\dagger \right), \end{aligned} \tag{A.2}$$

where the parameters M , M_S , M_Φ and M_3 are around or above the TeV scale. The model has an accidental Z_2 symmetry under which all the SM model particles are even while the new ones are odd. This symmetry prevents any tree-level generation of the higher dimensional operators when the heavy particles are integrated out. The operator \mathcal{O}_{HG} cannot be generated at one-loop since the colored particle does not couple to the Higgs. On the contrary, the equivalent operator for the photon cannot be avoided. Indeed, even if the fermions can be chosen to be neutral, all the new scalars cannot be simultaneously neutral. The constraints from gluon fusion in the low mass will change with the branching ratio to two photons. Nevertheless, the chromomagnetic operator is induced at one-loop and its coefficient given by

$$\frac{c_{hg}}{\Lambda^2} = \frac{\kappa \beta g_s M_3}{4(4\pi)^2 M^3} \left[\frac{R_\Phi^2 (1 - 3R_S^2) + R_S^2 + 1}{(R_\Phi^2 - 1)^2 (R_S^2 - 1)^2} + \frac{4 \left(\frac{R_S^4 \log(R_S)}{(R_S^2 - 1)^3} - \frac{R_\Phi^4 \log(R_\Phi)}{(R_\Phi^2 - 1)^3} \right)}{R_\Phi^2 - R_S^2} \right] \tag{A.3}$$

where $R_S \equiv \frac{M_S}{M}$ and $R_\Phi \equiv \frac{M_\Phi}{M}$.

Open Access. This article is distributed under the terms of the Creative Commons Attribution License which permits any use, distribution and reproduction in any medium, provided the original author(s) and source are credited.

References

- [1] UTFIT collaboration, M. Bona et al., *Model-independent constraints on $\Delta F = 2$ operators and the scale of new physics*, *JHEP* **03** (2008) 049 [[arXiv:0707.0636](#)] [[INSPIRE](#)].
- [2] Z. Han and W. Skiba, *Effective theory analysis of precision electroweak data*, *Phys. Rev. D* **71** (2005) 075009 [[hep-ph/0412166](#)] [[INSPIRE](#)].
- [3] R. Barbieri, A. Pomarol, R. Rattazzi and A. Strumia, *Electroweak symmetry breaking after LEP-1 and LEP-2*, *Nucl. Phys. B* **703** (2004) 127 [[hep-ph/0405040](#)] [[INSPIRE](#)].
- [4] C. Zhang, N. Greiner and S. Willenbrock, *Constraints on non-standard top quark couplings*, [arXiv:1201.6670](#) [[INSPIRE](#)].
- [5] C. Degrande, J.-M. Gerard, C. Grojean, F. Maltoni and G. Servant, *Non-resonant new physics in top pair production at hadron colliders*, *JHEP* **03** (2011) 125 [[arXiv:1010.6304](#)] [[INSPIRE](#)].
- [6] J.F. Kamenik, M. Papucci and A. Weiler, *Constraining the dipole moments of the top quark*, *Phys. Rev. D* **85** (2012) 071501 [[arXiv:1107.3143](#)] [[INSPIRE](#)].
- [7] D. Carmi, A. Falkowski, E. Kuflik and T. Volansky, *Interpreting LHC Higgs results from natural new physics perspective*, [arXiv:1202.3144](#) [[INSPIRE](#)].
- [8] A. Azatov, R. Contino and J. Galloway, *Model-independent bounds on a light Higgs*, *JHEP* **04** (2012) 127 [[arXiv:1202.3415](#)] [[INSPIRE](#)].
- [9] J. Espinosa, C. Grojean, M. Muhlleitner and M. Trott, *Fingerprinting Higgs suspects at the LHC*, *JHEP* **05** (2012) 097 [[arXiv:1202.3697](#)] [[INSPIRE](#)].
- [10] P.P. Giardino, K. Kannike, M. Raidal and A. Strumia, *Reconstructing Higgs boson properties from the LHC and Tevatron data*, *JHEP* **06** (2012) 117 [[arXiv:1203.4254](#)] [[INSPIRE](#)].
- [11] J. Ellis and T. You, *Global analysis of experimental constraints on a possible Higgs-like particle with mass ~ 125 GeV*, [arXiv:1204.0464](#) [[INSPIRE](#)].
- [12] A. Azatov, R. Contino, D. Del Re, J. Galloway, M. Grassi, et al., *Determining Higgs couplings with a model-independent analysis of $H \rightarrow \gamma\gamma$* , [arXiv:1204.4817](#) [[INSPIRE](#)].
- [13] M. Farina, C. Grojean and E. Salvioni, *(Dys)Zphilia or a custodial breaking Higgs at the LHC*, [arXiv:1205.0011](#) [[INSPIRE](#)].
- [14] W. Buchmüller and D. Wyler, *Effective Lagrangian analysis of new interactions and flavor conservation*, *Nucl. Phys. B* **268** (1986) 621 [[INSPIRE](#)].
- [15] B. Grzadkowski, M. Iskrzynski, M. Misiak and J. Rosiek, *Dimension-six terms in the standard model Lagrangian*, *JHEP* **10** (2010) 085 [[arXiv:1008.4884](#)] [[INSPIRE](#)].
- [16] G. Buchalla and O. Catà, *Effective theory of a dynamically broken electroweak standard model at NLO*, [arXiv:1203.6510](#) [[INSPIRE](#)].
- [17] G. Giudice, C. Grojean, A. Pomarol and R. Rattazzi, *The strongly-interacting light Higgs*, *JHEP* **06** (2007) 045 [[hep-ph/0703164](#)] [[INSPIRE](#)].

- [18] A.V. Manohar and M.B. Wise, *Modifications to the properties of the Higgs boson*, *Phys. Lett. B* **636** (2006) 107 [[hep-ph/0601212](#)] [[INSPIRE](#)].
- [19] A. Pierce, J. Thaler and L.-T. Wang, *Disentangling dimension six operators through di-Higgs boson production*, *JHEP* **05** (2007) 070 [[hep-ph/0609049](#)] [[INSPIRE](#)].
- [20] CDF AND D0 collaboration, T. Aaltonen et al., *Combined CDF and D0 upper limits on standard model Higgs boson production with up to 8.2fb^{-1} of data*, [arXiv:1103.3233](#) [[INSPIRE](#)].
- [21] ATLAS collaboration, *Combination of Higgs boson searches with up to 4.9fb^{-1} of pp collisions data taken at a center-of-mass energy of 7 TeV with the ATLAS experiment at the LHC*, [ATLAS-CONF-2011-163](#) (2011).
- [22] CMS collaboration, *Combination of SM Higgs searches*, [PAS-HIG-11-032](#) (Combination of SM Higgs Searches).
- [23] ATLAS collaboration, G. Aad et al., *Combined search for the standard model Higgs boson using up to 4.9fb^{-1} of pp collision data at $\sqrt{s} = 7\text{ TeV}$ with the ATLAS detector at the LHC*, *Phys. Lett. B* **710** (2012) 49 [[arXiv:1202.1408](#)] [[INSPIRE](#)].
- [24] LHC HIGGS CROSS SECTION WORKING GROUP collaboration, S. Dittmaier et al., *Handbook of LHC Higgs cross sections: 1. Inclusive observables*, [arXiv:1101.0593](#) [[INSPIRE](#)].
- [25] D. Choudhury and P. Saha, *Higgs production as a probe of anomalous top couplings*, [arXiv:1201.4130](#) [[INSPIRE](#)].
- [26] I. Low and A. Vichi, *On the production of a composite Higgs boson*, *Phys. Rev. D* **84** (2011) 045019 [[arXiv:1010.2753](#)] [[INSPIRE](#)].
- [27] J. Aguilar-Saavedra, *A minimal set of top-Higgs anomalous couplings*, *Nucl. Phys. B* **821** (2009) 215 [[arXiv:0904.2387](#)] [[INSPIRE](#)].
- [28] E. Cervero and J.-M. Gerard, *Minimal violation of flavour and custodial symmetries in a vectophobic two-Higgs-doublet-model*, *Phys. Lett. B* **712** (2012) 255 [[arXiv:1202.1973](#)] [[INSPIRE](#)].
- [29] ATLAS collaboration, G. Aad et al., *Summary plot of top quark pair production cross-section*, <https://twiki.cern.ch/twiki/bin/view/AtlasPublic/TopPublicResults> (2012).
- [30] H. Georgi, *Generalized dimensional analysis*, *Phys. Lett. B* **298** (1993) 187 [[hep-ph/9207278](#)] [[INSPIRE](#)].
- [31] A. Manohar and H. Georgi, *Chiral quarks and the nonrelativistic quark model*, *Nucl. Phys. B* **234** (1984) 189 [[INSPIRE](#)].
- [32] D. Nomura, *Effects of top-quark compositeness on Higgs boson production at the LHC*, *JHEP* **02** (2010) 061 [[arXiv:0911.1941](#)] [[INSPIRE](#)].
- [33] C. Zhang and S. Willenbrock, *Effective-field-theory approach to top-quark production and decay*, *Phys. Rev. D* **83** (2011) 034006 [[arXiv:1008.3869](#)] [[INSPIRE](#)].
- [34] N.D. Christensen and C. Duhr, *FeynRules - Feynman rules made easy*, *Comput. Phys. Commun.* **180** (2009) 1614 [[arXiv:0806.4194](#)] [[INSPIRE](#)].
- [35] C. Degrande, C. Duhr, B. Fuks, D. Grellscheid, O. Mattelaer, et al., *UFO - The universal FeynRules output*, *Comput. Phys. Commun.* **183** (2012) 1201 [[arXiv:1108.2040](#)] [[INSPIRE](#)].

- [36] P. de Aquino, W. Link, F. Maltoni, O. Mattelaer and T. Stelzer, *ALOHA: automatic libraries of helicity amplitudes for Feynman diagram computations*, [arXiv:1108.2041](#) [INSPIRE].
- [37] J. Alwall, M. Herquet, F. Maltoni, O. Mattelaer and T. Stelzer, *MadGraph 5 : going beyond*, *JHEP* **06** (2011) 128 [[arXiv:1106.0522](#)] [INSPIRE].
- [38] W. Beenakker, S. Dittmaier, M. Krämer, B. Plumper, M. Spira, et al., *Higgs radiation off top quarks at the Tevatron and the LHC*, *Phys. Rev. Lett.* **87** (2001) 201805 [[hep-ph/0107081](#)] [INSPIRE].
- [39] S. Dawson, L. Orr, L. Reina and D. Wackerroth, *Associated top quark Higgs boson production at the LHC*, *Phys. Rev.* **D 67** (2003) 071503 [[hep-ph/0211438](#)] [INSPIRE].